Annals of Nuclear Energy 141 (2020) 107290

Contents lists available at ScienceDirect

Annals of Nuclear Energy

journal homepage: www.elsevier.com/locate/anucene

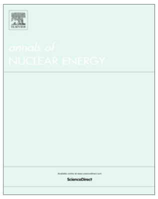

Uncertainty quantification of in-pool fission product retention during BWR station BlackOut sequences

Luis E. Herranz *, Carlos Aguado, Francisco Sánchez

Centro de Investigaciones Energéticas, Medioambientales y Tecnológicas (CIEMAT), Avda. Complutense, 40, 28040 Madrid, Spain

ARTICLE INFO

Article history:
Received 2 October 2019
Received in revised form 19 December 2019
Accepted 23 December 2019
Available online 5 January 2020

Keywords:
Fukushima Unit 1
Pool scrubbing
Uncertainty assessment

ABSTRACT

Suppression pools are an essential passive system for source term attenuation in boiling water reactors during severe accidents, particularly during Station BlackOut (SBO) sequences, as it happened in Fukushima.

This paper investigates how uncertain predictions of suppression pools decontamination can be. Based on MELCOR 2.1 calculations of Fukushima Unit 1, a stand-alone version of SPARC-90 (Suppression Pool Aerosol Removal Code) has been used in combination with DAKOTA-6.4, to propagate the uncertainties in the input deck variables affecting the Decontamination Factor (DF). The results indicate that DF uncertainties may spread around two orders of magnitude and the uncertainty margin stays roughly constant over time. In addition, a sensitivity analysis based on the Pearson and Spearman correlation coefficients has been carried out and pointed that uncertainties associated to particle inertia (i.e., particle density and size) and in-pool phase change (i.e., non-condensible gas fraction in the carrier gas) dominate the uncertainties found in the DF for this specific scenario.

1. Introduction

Suppression pools are an essential system in boiling water reactors during severe accidents, particularly during Station BlackOut (SBO) sequences, in which active safeguards cannot be relied upon. Their two-fold role as a sink of decay and chemical heat and as a passive trap for fission products (FP) and aerosols (i.e., pool scrubbing), makes its performance critical for the SBO accident evolution, as it was the case during the Fukushima accidents (Nuclear Emergency Response Headquarters, 2011).

Pool scrubbing (i.e., the removal of aerosol particles and vapors in gas bubbles moving through a water pool) provides a means to reduce source term to the environment during severe accidents (Allelein et al., 2009). Based on the different nature of hydrodynamic and vapor/aerosol phenomena governing the pool scrubbing decontamination, the carrier gas pathway through the aqueous volume is split into three regions (Fischer, 1998): injection, rise and pool surface. At the injection zone in the pool, the mechanical as well as the thermal gas–liquid interaction determine the scrubbing process; the gas composition and velocity are key variables in this region. During gas rise through the pool, hydrodynamics heavily affects scrubbing efficiency; liquid–gas exchange surface area and internal gas circulation velocity are examples of variables affecting particle retention mechanisms (i.e., inertial and centrifugal deposition) that might play a role during gas rise in the pool; besides, the gas residence time within the pool is strongly dependent on hydrodynamics. At the pool surface, bubbles rupture causes micro-droplets that might transport very fine aerosol particles as well as dissolved fission products get into the atmosphere (Herranz et al., 2014).

In the 80′s last century, stand-alone codes encapsulating these phenomena were built; they have been traditionally called pool scrubbing codes. The SPARC-90 code was one of such developments and its formulation was heavily based on experiments conducted in the early 80′s (Owczarski and Burk, 1991). In short, SPARC-90 estimates the in-pool decontamination resulting from mechanisms like diffusiophoresis, inertial impaction, centrifugal deposition and some others. SPARC-90, like other similar codes, were partially validated at the time and then embedded in integral severe accident analysis tools, like MELCOR (Humphries et al., 2015a, 2015b) or ASTEC (Chatelard et al., 2014). However, pool scrubbing modelling has been demonstrated to be far from being mature and further work has been found to be necessary (Herranz et al., 2014), so that a vast international project has been built to address this issue (Gupta et al., 2017) in the frame of NUGENIA (www.nugenia.org).

Beyond modelling maturity, uncertainties affecting highly influencing variables on pool scrubbing might result in large

---

* Corresponding author.

https://doi.org/10.1016/j.anucene.2019.107290
0306-4549/

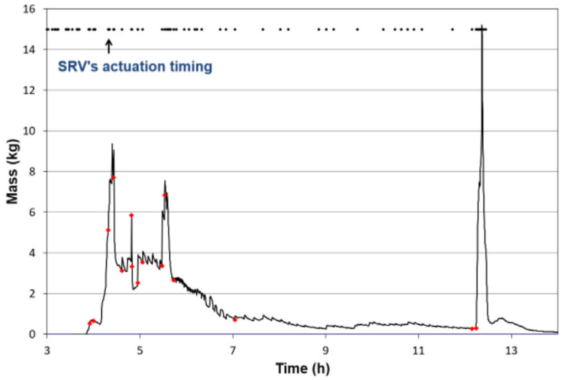

Fig. 1. RPV airborne aerosol mass.

uncertainties in the estimates of decontamination capability, particularly at high levels of in-pool retention (i.e., minor efficiency variations at high Decontamination Factor (DF) values, around 10^2, result in changes of orders of magnitude in DF). An assessment of such DF uncertainty band during an SBO accident sequence in a BWR3 Mark I reactor is the objective of this paper. To do so, based on MELCOR 2.1 calculations of Fukushima Unit 1 (Herranz and López, 2018), a stand-alone version of SPARC-90 (Owczarski and Burk, 1991) has been used in combination with DAKOTA-6.4 (Adams et al., 2014) to propagate the uncertainties in the input deck variables affecting the DF.

Finally, it is worth nothing that source term uncertainties, as a whole, might have a high impact on practical aspects, like accident management and, no less important, emergency preparedness. However, given the high complexity of applying Best Estimate Plus Uncertainty (BEPU) methods in the severe accident arena, a systematic application of BEPU has not been attempted yet, although a few pioneering works were done in the past (Herranz and Gauntt, 2018). Presently, there are international initiatives just started under different frameworks, as the EC-MUSA project launched within the EC H2020 Program (Herranz and Paci, 2019).

2. The SBO scenario

Modelling of the SBO accident in Unit 1 of Fukushima with MELCOR 2.1 (Herranz and López, 2018), resulted in airborne particles mass in the RPV (Reactor Pressure Vessel) dome. Fig. 1 shows its evolution along time (SRV opening times also displayed). Their transport to the suppression pool through the Safety Relief Valves (SRV) is characterized by a set of variables, the most important of which (i.e., particle size distribution, gas mass flow rate and composition) are shown in Fig. 2. These, together with those

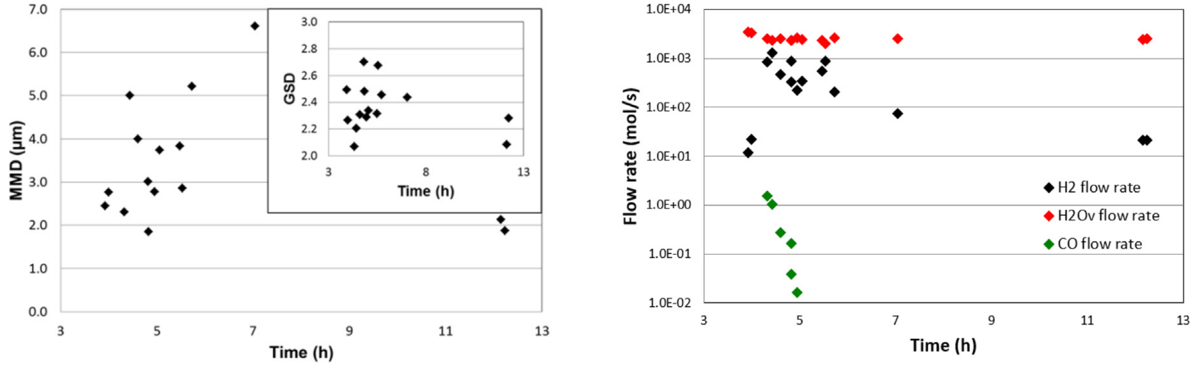

a. Particle size distribution

b. Carrier gases

Fig. 2. Main characteristics of in-pool injection materials.

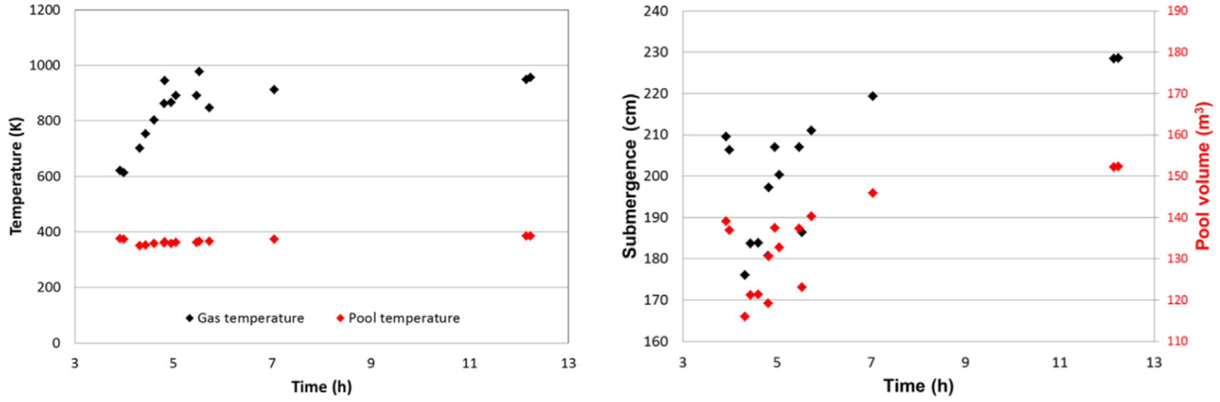

a. Temperature

b. Pool submergence

Fig. 3. Suppression pool characterization during particle injection.

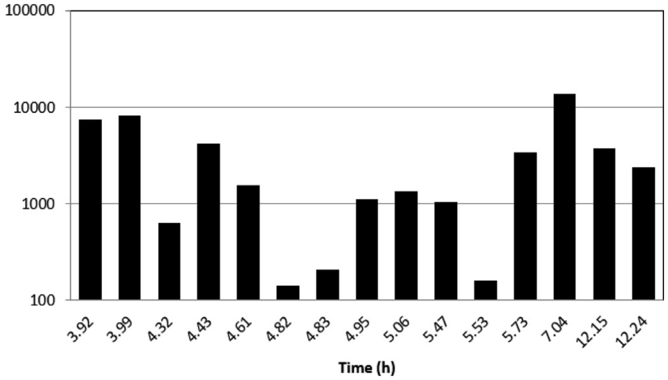

Fig. 4. DFs predicted during the FP injection in the suppression pool.

Table 2
Uncertainty bounds.

	Variable	Lower bound	Upper bound
INJECTION DEPTH	Submergence	−10%	+10%
	Pool volume	−10%	+10%
THERMALHYDRAULICS	Pool temperature	-(T_{N1}-T_{Ncold})/2	+(T_{N1}-T_{Ncold})/2
	Pool pressure	−10%	+10%
	Gas temperature	−30%	+30%
	Gas pressure	−5%	+5%
CARRIER GASES	H_2 mass flow rate	−100%	100%
	H_2Ov mass flow rate	−10%	+10%
	CO mass flow rate	−50%	+50%
PARTICLES	MMD	−50%	+50%
	GSD	−20%	+20%
	Total particles mass flow rate	−100%	+100%
	Particles density	−67%	+67%

Table 1
Input variables.

Variable	Units	4.61 h	4.83 h
MMD	µm	3.99	1.85
GSD	–	2.309	2.481
H_2 molar flow rate	mol/s	468.3	328.7
H_2Ov molar flow rate	mol/s	2500	2340
CO molar flow rate	mol/s	0.27	0.04
Pool temperature	K	357.5	363.6
Gas temperature	K	802.3	945.1
Pool volume	m^3	121.3	130.6
Submergence	m	1.84	1.97

characterizing the pool status (i.e., subcooling and submergence; Fig. 3) determine to a good extent the decontamination capability of the pool. In order to describe the whole transient from the onset of fission product release from fuel during core degradation to the time at which RPV fails, a total of 15 time points have been chosen (red dots in Fig. 1).

An aspect of the scenario modeling that heavily affected the MELCOR estimates of the variables involved in pool scrubbing was the wetwell (W/W) model. The entire W/W system was split into 8 circumferential nodes (one per each vent connecting drywell -D/W- and W/W) and it was assumed a "perfect axial stratification", which means that the water layer below the injection point was not considered (i.e., the pool heat capacity was significantly reduced). The effect of such an approximation on the thermal evolution of the suppression pool was discussed by Herranz et al. (2015).

Some of the boundary conditions heavily affecting pool scrubbing show large variations in short time periods. This is the case of the particle size (Mass Median Diameter, MMD), which doubles (from about 2.2 to 5.0 µm) between 4.32 h and 4.43 h. This would strongly enhance the efficiency of inertial deposition mechanisms within the pool. Another example is the carrier gas composition. Fig. 2b shows that gas composition is dominated by steam, but non-condensible gases (mostly H_2; CO produced through oxidation of B_4C is never significant) can reach molar fractions around 33%, which would noticeably reduce the condensing potential of the gas when entering the subcooled pool (water temperature was well below the saturation temperature over most of injection period). Other variables, like pool submergence did not show major variations over the interval under analysis. Finally, a rather steady high gas velocity (jet injection regime) was predicted all over the time.

In addition, it should be noted that when transferring MELCOR information into SPARC-90 input deck, some of the above variables undergo some adaptation. Particle size, for instance, has been described in SPARC-90 as a size distribution consisting of 20 bins. The major hypotheses in SPARC-90 simulations are listed below:

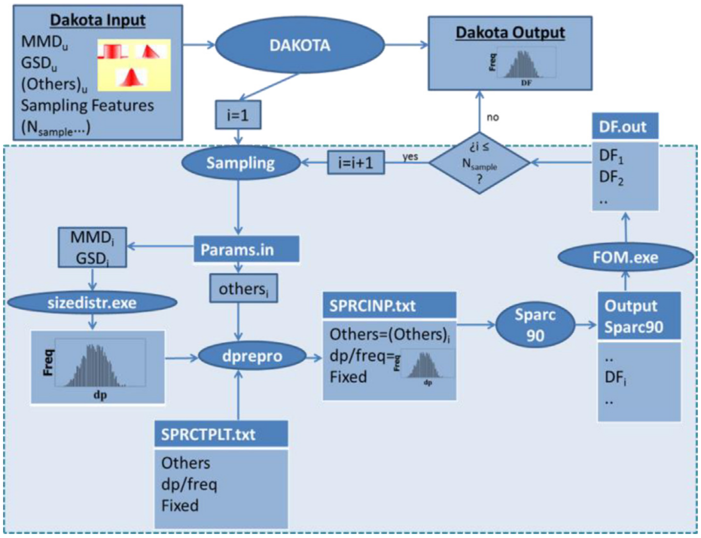

Fig. 5. Flowchart of the UQ methodology.

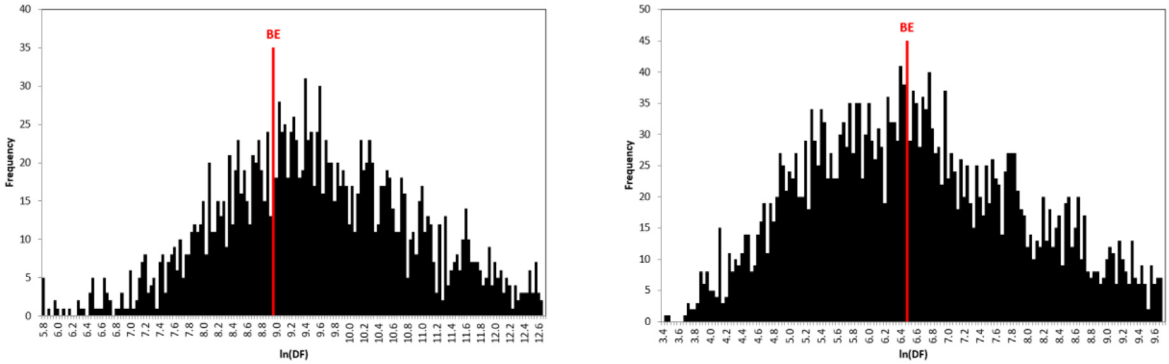

a. 3.92 h b. 4.32 h

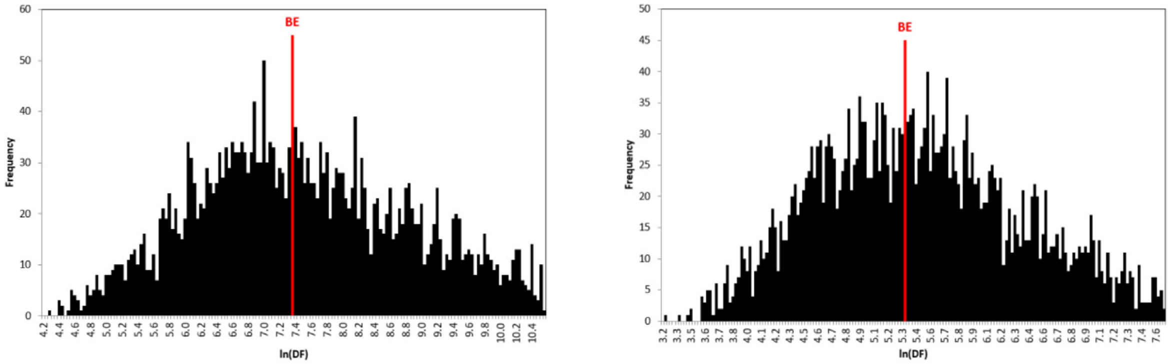

c. 4.61 h d. 4.83 h

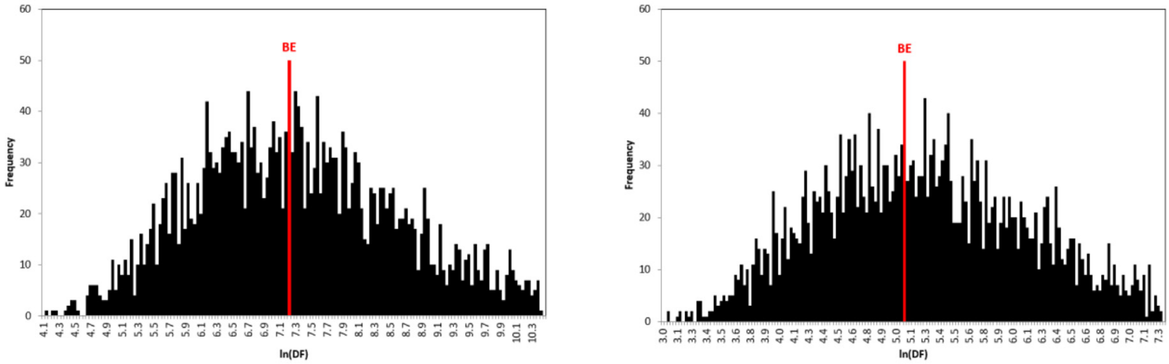

e. 5.06 h f. 5.53 h

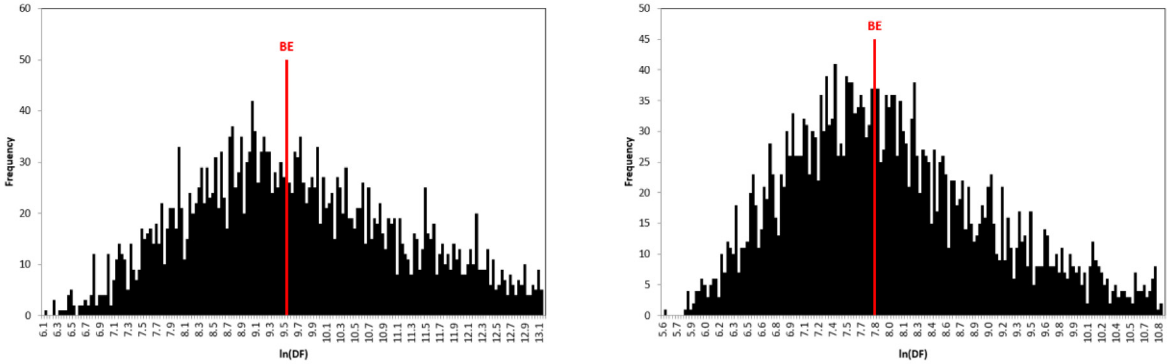

g. 7.04 h h. 12.24 h

Fig. 6. DF distributions.

- Particle size distribution is assumed to be lognormal; the entire distribution was derived from the MELCOR estimates of MMD and GSD (Geometric Standard Deviation).
- Gas injection was postulated to uniformly distribute across the more than thousand 1 cm holes of the T-quencher injector; namely, pressure and mass losses in the T-quencher were neglected.
- Particle density was approximated as 3000 kg/m^3.
- Gas thermal state at the pool inlet was taken as the one at the RPV dome (i.e., adiabatic transport through the piping assumed).

The DF results obtained in the 15 red-color points noted in Fig. 1 are shown in Fig. 4 (hereafter referred to as Best Estimates, BE). As observed, at all times during the aerosol transport into the suppression pool the decontamination capability has been over 100 (i.e., scrubbing efficiencies higher than 99%). It has been already discussed elsewhere that DFs over 100 become very sensitive to uncertainties in the retention efficiency and caution should be taken if they are to be credited (Herranz, 2009). Therefore, even if large DF changes are observed in consecutive times, they do not mean such abrupt changes in terms of mass.

Out of the 15 time points, two specific times (4.61 h and 4.83 h) have been chosen in this study, one with DF over 10^3 and the other one, an order of magnitude less, so that a wide range is covered. Table 1 provides the quantitative boundary conditions of them.

3. The uncertainty quantification methodology

Fig. 5 shows a diagram of the uncertainty quantification methodology based on the DAKOTA 6.4 software. In addition to the sampling size, the DAKOTA input deck is fed with the lower and upper bounds of the uncertain variables and the Probability Density Function (PDF) describing the evolution within the interval. Given the lack of information concerning PDF's in the case under study, uniform distributions have been assumed. Once the uncertainty domains of SPARC-90 input variables have been sampled through a Monte Carlo calculation, the particle size distribution is developed from the MMD and the GSD resulting from the sampling. The sampling size for each time point analysis has been set to 3000, which according to Wilks theorem assures that more than 99% of the population lies between the upper and lower bounds of the distribution obtained with a 99% of confidence (Wilks, 1941).

The determination of the input variables uncertainties has been heavily based on technically supported engineering judgement. The variability of some of those magnitudes, stemming from the intermittent performance of SRV's, has been assessed by analyzing their values at an earlier and at a later time step. Based on this information and the experience of the authors simulating severe accident scenarios, Table 2 has been set up. The criteria adopted to set the upper and lower bounds of the uncertainty domain, are the following:

- By default, the maximum difference with respect to previous and later time steps in MELCOR has been chosen (their specific value is given in relative terms in Table 2).
- The pool temperature uncertainty range has been set as half the difference between the coldest (T_{Ncold}) and hottest (T_{N1}) circumferential locations in the pool.
- As for particle density, the lower bound has been set to be the water density (1000 kg/m^3) and, correspondingly, the upper one has been a 67% higher than the BE value.
- Given the high fluctuations in the particle concentration at the RPV dome, a 100% uncertainty has been set.

Uncertainties of injection depth and most thermalhydraulics variables are moderate; pool temperature, though, shows significant uncertainties. Contrarily, variables like H_2 content in the carrier gas or MMD and density have shown a noticeable uncertainty.

The DF uncertainty estimates to be presented in the next section is the result of the uncertainties in the input-deck variables. Namely, other sources of uncertainties have not been accounted for. Hence, the results should be understood as a minimum width of the uncertainty band. Uncertainties associated to lack and/or drawbacks of in-code models is not considered. Some of them, though, might affect estimates significantly, like the absence of jet regime and churn-turbulent models describing the gas behavior at the inlet and during bubble rise, respectively. In addition, there are some boundary conditions that are not properly described in current codes, even if they might heavily affect the gas dynamics and the actual gas decontamination in pools, like the presence of impurities (particularly surfactants) in the aqueous phase during the scrubbing process. Herranz et al. (2014) discussed these and other factors more extensively.

4. Results and discussion

4.1. Uncertainty analysis

In order to illustrate the results obtained in the uncertainty quantification, Fig. 6 shows the distribution of about half of the 15 time points calculated in section 2. In this sample, DF best estimates spread over more than one order of magnitude (from 10^2 to over 10^3). The sample size of all of them was set to 3000 and the PDF defined as uniform (a random Monte Carlo method has been used for sampling). Note that 5% of DF calculations have been dropped at the upper bound of the distribution, so that the DF distribution shown corresponds to the 95% of the full sampling (IAEA, 2008).

As observed, all the uncertainty distributions are Gaussian-like in the ln(DF) domain (i.e., lognormal distributions in the DF domain), with the BE DF near the mode of the distribution, which might give some credit to the BE estimates. However, lower and upper bounds of DF draw the attention to the fact that one should expect an uncertainty band about 2 orders of magnitude or even broader. This should be a concern, particularly at the lower end of calculated DF BE (1 0 ^{2}). In terms of mass retained it would mean that estimates of just 1% of the incoming mass leaving the pool could be anything between 0.1% and 10%, which might entail drastic differences in terms of dose rates. Of course, the upper DF bound is less a safety concern, as it would always result in lower dose rates.

In addition, to further support the reliability of the results, the effect of several aspects of the methodology used on the uncertainty quantification has been investigated: sample size (3000 vs 10000); sampling method (random Monte Carlo – MC – vs Latin Hypercube Sampling – LHS –); and shape of the PDF chosen (uniform vs normal). Table 3 compiles the four alternative analyses to the base case done.

Table 3
Sensitivity matrix of the uncertainty methodology.

	Sample Size	Sampling Method	Input PDF shapes
Base Case	3000	MC	Uniform
Case 1	3000	MC	Normal (*)
Case 2	3000	LHS	Uniform
Case 3	3000	LHS	Normal (*)
Case 4	10,000	MC	Uniform

(*) In normal distributions the lower bound and the upper bound correspond to -3σ and $+3\sigma$, respectively.

Table 4
Uncertainty analysis results.

	Sampling and distribution	Best Estimate	Dakota – SPARC-90							
		DF	Mean DF	RD(%)	Median DF	RD(%)	DF max	RD(%)	DF min	RD(%)
4.61 h	Base Case	1580	4270	–	1580	–	37,100	–	72	–
	Case 1		1980	−53.6	1560	−1.3	6920	−81.3	176	144.4
	Case 2		4560	6.8	1620	2.5	43,700	17.8	69	−4.2
	Case 3		2010	−52.9	1550	−1.9	7150	−80.7	173	140.3
	Case 4		4426	3.7	1623	2.7	41,620	12.2	60	−16.7
4.83 h	Base Case	207	357	–	224	–	2070	–	25	–
	Case 1		235	−34.2	215	−4.0	549	−73.5	53	112.0
	Case 2		364	2.0	221	−1.3	2290	10.6	31	24.0
	Case 3		233	−34.7	212	−5.4	567	−72.6	43	72.0
	Case 4		373	4.5	227	1.3	2342	13.1	28	12.0

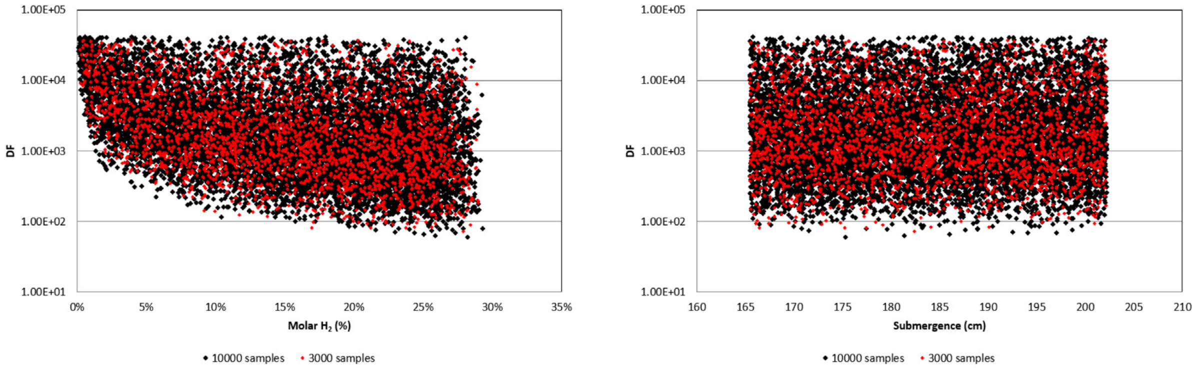

DF versus molar H_2

DF versus submergence

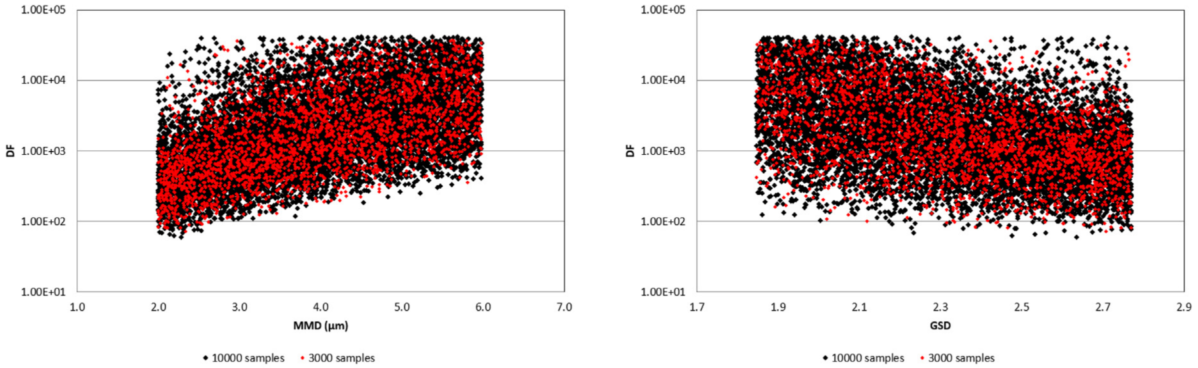

Df vs MMD

Df vs GSD

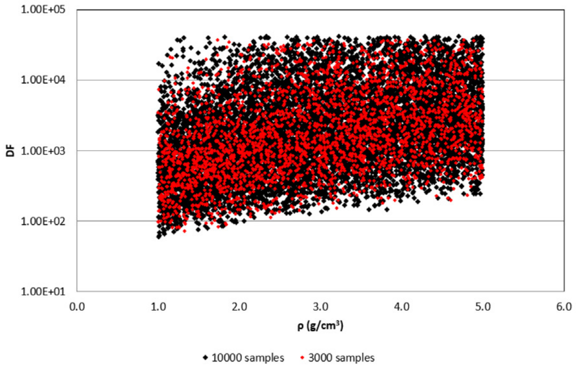

DF vs particle density

Fig. 7. DF uncertainty distributions.

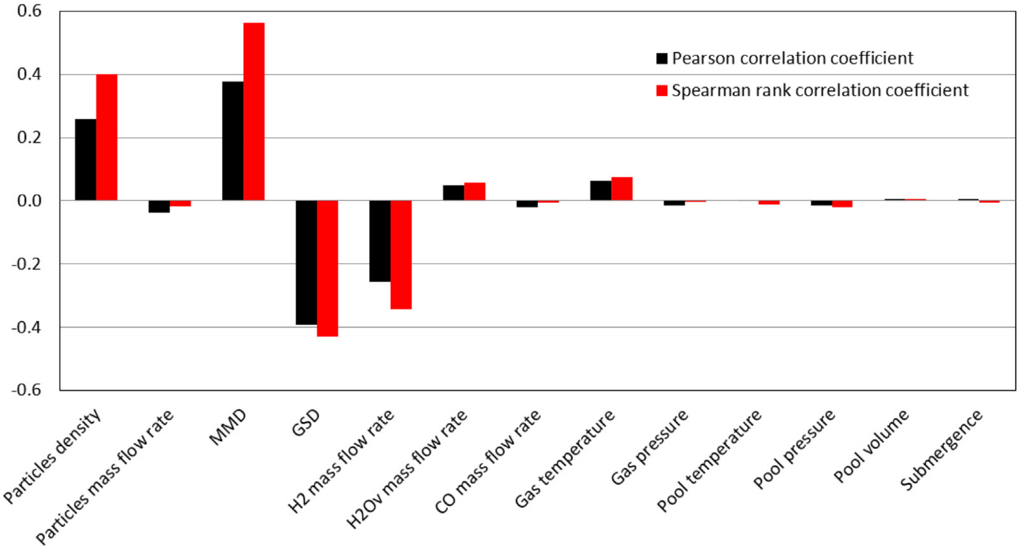

Fig. 8. Pearson and Spearman coefficient for DF for time point#5 MC uniform.

Table 4 collects the results of the sensitivity study in terms of DF mean, median, maximum and minimum. Both at moderate DF values (1 0 0) and high ones (1000), the sampling mode hardly influences the mean and median DF. Contrarily, the PDF type has a significant effect; except for the distribution median, the other features in Table 4 show noticeable differences when using uniform or gaussian PDF's. This is particularly true when establishing uncertainty limits, since for a better known probability distribution (such as a Gaussian distribution versus a uniform distribution) the associated uncertainty band is much narrower. In other words, a better characterization of uncertainties affecting the pool scrubbing boundary conditions would significantly reduce the DF uncertainties.

In order to further discuss the effect of the sample size, the distribution of DF calculations as a function of potential influencing variables of the decontamination process (i.e., H_2 fraction; submergence; and particle size and density) is shown in Fig. 7 for the case with DF BE over 10^3 (t = 4.61 h). No major differences are noted between them, the 10,000 case just showing few higher and lower values bounding the 3000 case. In addition, the uncertainty band width changes mildly over a broad variable range, so that the uncertainty scatter is not a strong function of the value adopted by the physical variable in the ranges explored. And, finally, the tendency (either increasing or decreasing) shown by the uncertainty band is consistent with the physics underneath (for example, the higher the H_2 fraction, the lower the DF because there is less condensation potential in the pool).

Finally, it should be highlighted that under the conditions prevailing in the SBO accident analyzed, no matter how broad is the uncertainty band an efficient fission products retention in the pool is estimated to occur so that most fission products, except for Noble Gases, is trapped in the water. In other cases, though, where a broad uncertainty band persisted and water was not a so efficient filter, the uncertainty band might translate in DFs indicating a substantial fraction of fission products going through the pool and posing a radiological threat wherever they move to eventually.

4.2. Sensitivity analysis

To determine the sensitivity of DF with the input variables, the Pearson correlation coefficient and the Spearman rank correlation coefficient are used (Ikonen and Tulkki, 2014). The first one determines the linearity of the relationship between DF and each of the input variables considered and the second one determines whether there is a correlation, either positive (both variables increasing) or negative (one variable increasing and one variable decreasing), or there is no correlation at all. Fig. 8 shows the results obtained.

It is noticeable that exists a strong dependence with particles density, MMD, GSD and H_2 mass flow rate. This is conveying a physically sound message: particle inertia at the inlet of the pool and drag by steam condensation are the dominant particle removal processes in the scenario analyzed and make suppression pool such a good fission product filter. At the inlet of the pool, while gas globule is growing until its detachment from the injector, big enough particles are submitted to their inertia, leave the internal gas streamlines and hit the bubble surface; in addition, those particles remaining in the gas circulation undergo deposition due to centrifugal forces. Both mechanisms depend on particle density and particle diameter squared (Hinds, 1999), which is captured in the sensitivity analyses above. As for H_2, the presence of a non-condensible gas drastically reduces the steam condensation rate (Chapman, 1984). Given the hypothesis of an instantaneous thermal equilibrium at the pool inlet in SPARC-90, any gas other than steam results in a reduction of steam condensation. Consequently, the amount of particles removed decreases proportionally, which explains the negative correlation between H_2 and DF.

5. Concluding remarks

This paper quantifies uncertainties in the decontamination capability estimates calculated with MELCOR 2.1 for a SBO sequence in a BWR3 Mark I containment. The resulting uncertainty intervals should be seen as a minimum since they encapsulate just those associated to the input variables in stand-alone pool scrubbing codes. Nevertheless, some important insights have been gained:

- DF uncertainty spreads over roughly two orders of magnitude, which given the high DF values might not have a major impact on source term predictions in the SBO sequence simulated, but they might have a significant safety impact on other accident sequences with not so efficient scrubbing in water ponds if a similar uncertainty band width was calculated.

- In the scenarios being analyzed, the major removal processes responsible for most of particle scrubbing are inertial and phase change (i.e., steam condensation) mechanisms. Both of them are heavily located at the pool inlet.

This study is specific to the scenario modeled and not a generic statement on pool scrubbing DF uncertainty width can be concluded. Nonetheless, it does illustrate how sensitive high DFs can be to slight changes in those variables dominating retention in the pool. Finally, it is worth emphasizing that uncertainty sources coming from the lack of suitable models for the conditions addressed (i.e., jet regime injection, churn-turbulent gas motion rising up through the pool, effect of substances other than water in the pool, etc.) have not been considered ; in other words, the actual uncertainty band should be expected to be broader.

Further work will proceed through the adaptation of the methodology used in this analysis to the uncertainties quantification in risk-dominant sequences. In fact, this work has been already initiated within the EU-MUSA project (Herranz and Paci, 2019).

CRediT authorship contribution statement

Luis E. Herranz: Conceptualization, Methodology, Writing - original draft, Supervision, Resources, Project administration, Funding acquisition, Investigation. **Carlos Aguado:** Software, Writing - review & editing. **Francisco Sánchez:** Formal analysis, Data curation, Visualization.

Declaration of Competing Interest

The authors declare that they have no known competing financial interests or personal relationships that could have appeared to influence the work reported in this paper.

Acknowledgement

The authors acknowledge partners of the NUGENIA/TA2 IPRESCA project for the technical discussions held while developing this work.

References

Adams B. M., Bohnhoff W. J., Dalbey K. R., Eddy J. P., Ebeida M. S., Eldred M. S., Hough P. D., Hu K. T., Jakeman J. D., Maupin K. A., Monschke J. A., Ridgway E. M., Ahmad Rushdi, Swiler L. P., Stephens J. A., Vigil D. M. and Wildey T. M., 2014. Dakota, a multilevel parallel object-oriented framework for design optimization, parameter estimation, uncertainty quantification, and sensitivity analysis: Version 6.4 user's manual. Technical Report SAND2014-4633, Sandia National Laboratories, Albuquerque, NM, Updated May, 2016.

Allelein H.J., Auvinen A., Ball J., Güntay S., Herranz L.E., Hidaka A., Jones A.V., Kissane M., Powers D., Weber G., 2009. State-of-the-art report on nuclear aerosols, NEA/CSNI/R(2009)5, 17-Dec-2009.

Chapman, A.J., 1984. Heat Transfer, 4th Edition, Ch. 10: Heat Transfer in Condensing and Boiling. Macmillan Publishing Company.

Chatelard, P., Reinke, N., Arndt, S., Belon, S., Cantrel, L., Carenini, L., Chevalier-Jabet, K., Cousin, F., Eckel, J., Jacq, F., Marchetto, C., Mun, C., Piar, L., 2014. ASTEC V2 severe accident integral code main features, current V2.0 modelling status, perspectives. Nucl. Eng. Des. 272, 119–135.

Fischer K., 1998. Model uncertainties and development for aerosol pool scrubbing, third OECD Specialist Meeting on Nuclear Aerosols in Reactor Safety, Cologne (Germany) June 15–18.

Gupta S., Herranz L.E., Van Dorsselaere J-P, 2017. Integration of Pool scrubbing Research to Enhance Source-term Calculations (IPRESCA). 8th European Review Meeting on Severe Accident Research - ERMSAR-2017 Warsaw, Poland, 16–18 May 2017.

Herranz L.E., Tardáguila R.D., Berschart T., Lind T., Morandi S., 2014. Remaining issues in pool scrubbing: major drivers for experimentation within the EU-PASSAM project. Proceedings of ICAPP 2014, Charlotte (USA), April 6–9.

Herranz, L.E., Fontanet J., 2009. Assessment of ASTEC-CPA pool scrubbing models against POSEIDON-II and SGTR-ARTIST data. Proceedings of ICAPP'09.

Herranz, L.E., Fontanet, J., Fernández, E., López, C., 2015. Influence of the wet-well nodalization of a BWR3 Mark I on the containment thermal-hydraulic response during an SBO accident. Nucl. Eng. Design 295 (2015), 138–147.

Herranz L.E., López C., 2018. Progress in understanding Fukushima Unit 1 severe accident through a forensic analysis with MELCOR. Proceedings of ICAPP 2018, Charlotte (USA), April 8–11.

Herranz L.E., Gauntt R.O., 2018. Historical Overview of Severe Accident Analysis and the Need for Uncertainty Quantification. Key-Note lecture. In: "Best Estimate Plus Uncertainty International Conference". Lucca (Italy), May 13–18.

Herranz L.E., Paci S., 2019. MUSA: Management and Uncertainties of Severe Accidents. Poster. In: "9th European Commission Conference on EURATOM Research and Training in Safety of Reactor Systems (FISA 2019)". Pitesti (Romania), June 4–7.

Hinds, W.C., 1999. Aerosol Technology: Properties, Behavior and Measurement of Airborne Particles. 2nd Ed., Ch. 3 and Ch. 5, A. Wiley-Interscience Publication, John Wiley & Sons Inc.

Humphries L.L., Cole R.K., Louie D.L., Figueroa V.G., Young M.F., 2015a. MELCOR Computer Code Manuals, Vol. 1: Primer and Users' Guide, Version 2.1.6840, SAND 2015-6691 R, Sandia National Laboratories, August, 2015.

Humphries L.L., Cole R.K., Louie D.L., Figueroa V.G., Young M.F., 2015b. MELCOR Computer Code Manuals, Vol. 2: Reference Manual, Version 2.1.6840, SAND 2015-6692 R, Sandia National Laboratories, August, 2015.

IAEA, 2008. Best Estimate Safety Analysis for Nuclear Power Plants: Uncertainty Evaluation, Safety Report Series, No. 52.

Ikonen, T., Tulkki, V., 2014. The importance of input interactions in the uncertainty and sensitivity analysis of nuclear fuel behavior. Nucl. Eng. Design 275 (2014), 229–241.

Nuclear Emergency Response Headquarters, 2011. Report of the Japanese Government to the IAEA Ministerial Conference on Nuclear Safety – The Accident at TEPCO's Fukushima Nuclear Power Stations. June 2011.

Owczarski P.C., Burk K.W., 1991. SPARC-90: A Code for Calculating Fission Product Capture in Suppression Pools. Prepared for Division of Regulatory Applications Office of Nuclear Regulatory Research, U.S. Nuclear Regulatory Commission. NUREG/CR-5765.

Wilks, S.S., 1941. Determination of sample sizes for setting tolerance limits. Ann. Math. Stat. 12 (1941), 91–96.